

Tidal Stripping of Globular Clusters in the Virgo Cluster

Valeria Coenda¹, Hernán Muriel¹

*Instituto de Investigaciones en Astronomía Teórica y Experimental IATE, Observatorio
Astronómico OAC, Laprida 854, X5000BGR, Córdoba, Argentina.*

vcoenda@oac.uncor.edu, hernan@oac.uncor.edu

and

Carlos Donzelli^{1,2}

*Space Telescope Science Institute, 3700 San Martin Drive, Baltimore, MD 21218, USA.
IATE, OAC, Argentina.*

donzelli@stsci.edu

Abstract

With the aim of finding evidence of tidal stripping of globular clusters (GCs) we analysed a sample of 13 elliptical galaxies taken from the ACS Virgo Cluster Survey (VCS). These galaxies belong to the main concentration of the Virgo cluster (VC) and present absolute magnitudes $-18.5 < M_z < -22.5$. We used the public GC catalog of Jordán et al. (2008) and separated the GC population into metal poor (blue) and metal rich (red) according to their integrated colors. The galaxy properties were taken from Peng et al. (2008). We found that:

1) The specific frequencies (S_N) of total and blue GC populations increase as a function of the projected galaxy distances r_p to M87. A similar result is observed when 3-dimensional distances r_{3D} are used. The same behaviours are found if the analysis are made using the number of GCs per $10^9 M_\odot$ (T). No correlations between S_N or T and r_p or r_{3D} is observed for the red GC population. The correlations for the blue GCs (typically more extended) and the lack of correlations for the red GCs (more concentrated) with the clustocentric distance of the host galaxy are interpreted as evidence of GCs stripping due to tidal forces.

¹ Consejo Nacional de Investigaciones Científicas y Técnicas (CONICET), Avenida Rivadavia 1917, C1033AAJ, Buenos Aires, Argentina.

²AURA US Gemini Fellow

2) No correlation is found between the slope of GC density profiles of host galaxies and the galaxy distance to M87 (Virgo central galaxy). The lack of such a correlation is interpreted in terms of a shrinkage of the GC distribution after the stripping of GCs in the outermost region of galaxies.

3) We also computed the local density of GCs (ρ_{out}) located further than 6.2 kpc from the galaxy center for nine galaxies of our sample. We find that the GC population around most of these galaxies is mainly composed of blue GCs. The two highest values of ρ_{out} are found in the core of the VC (up to 100 kpc) and correspond to the two lowest values of S_N .

Our results suggest that the number and the fraction of blue and red GCs observed in elliptical galaxies located near the centers of massive clusters, could be significantly different from the underlying GC population. These differences could be explained by tidal stripping effects that occur as galaxies approach the centers of clusters.

Subject headings: galaxies: clusters: general — galaxies: elliptical and lenticular, cD — galaxies: interactions — Galaxy: globular clusters: general

1. Introduction

It has been demonstrated that tidal interactions can strongly affect the evolution of galaxies in clusters. Rapid gravitational encounters (galaxy harassment) as well as the global gravitational field of the cluster itself can dramatically change galaxy properties. Some of the properties that can be affected by tidal forces are those related to the population of globular clusters (GCs). Muzzio and collaborators in the 80s (Muzzio 1986, Muzzio et al. 1987), and more recently Bekki et al. (2003, hereafter B2003), used collisionless dynamical simulations to demonstrate that galaxies in clusters can lose a significant fraction of their GC population as a consequence of tidal stripping. Moreover, since the outermost regions of a galaxy are more sensitive to tidal effects, B2003 found that the number density profile of the GC population becomes steeper after the stripping. In addition, given that tidal encounters as well as the global effect of the cluster potential increase towards the inner region of the cluster, a positive correlation between the slope of the density profile of the GC population and the clustocentric distance of the galaxies is expected to be observed.

If GCs are stripped from galaxies, a fraction of these GC should populate the intracluster medium. Bekki & Yahagi (2006, hereafter BK2006) investigated the spatial distribution of intracluster GCs (ICGC) using high-resolution cosmological simulations, and found that

ICGC population contribute 20-40% to the total GC population in high mass clusters, making the case for an inhomogeneous, asymmetric and elongated distribution.

It is well known that color distributions of GCs are typically bimodal (Peng et al. 2006), indicating two sub-populations of GCs. Spectroscopic studies have shown that color bimodality is mainly due to differences in the metallicity of the two sub-populations: the metal-poor GCs are blue, while the metal-rich GC are red. Blue GCs present a shallower and more extended radial density profile than red GCs, and consequently have a higher probability to be stripped from the parent galaxy. In the tidal stripping scenario, the cluster core and, therefore, the central galaxy play an important role. For example, Forte et al. (1982) found that the properties of the GC population in M87 (Virgo central galaxy) are consistent with the accretion of GCs from less massive galaxies. Côté et al. (1998) explored the possibility that the metal-poor population of giant elliptical galaxies arises from the capture of GC from other galaxies. Analysing the two brightest galaxies in Virgo, these authors concluded that it is possible to explain the observed properties of the blue GC population in M49 and M87 without invoking new GC formation through mergers or multiple bursts.

Forbes et al. (1997) found evidence of tidal stripping in Fornax. These authors analyzed the specific frequency of GCs in four galaxies located in central cluster regions and found a marginal dependence of S_N (the number of GCs scaled to the galaxy luminosity) on the clustocentric galaxy distance r_c . Nevertheless, the r_c range considered is relatively small ($r_c < 200\text{kpc}$). The same cluster was also analysed by Hilker et al. (1999). These authors suggested that an important fraction of the GC population of the cD galaxy NGC 1399 could be explained by GCs stripped from the central giant galaxies making those central galaxies to present low specific frequencies. In order to quantify the importance of the tidal stripping effect, it is fundamental to study new clusters of galaxies and also to extend the limited range of clustocentric distances currently available. Recently, Peng et al. (2008, hereafter P2008) studied the formation efficiencies of GCs in the Virgo Cluster Catalog (VCC) sample. They found that both, high and low luminosity early type galaxies, have large S_N values, while those galaxies with intermediate luminosities ($-20 < M_B < -17$) present small and relatively constant S_N . They also found that S_N depends on the environment, i.e. 1) galaxies within a projected radius of 1 Mpc from the cluster center tend to have higher GC fractions, and 2) galaxies within $r_p \simeq 40\text{kpc}$ of M87 (and M49) have few or no GCs. The first result is interpreted in terms of the formation time, where GCs formation in central dwarf galaxies is biased because their stars form earlier; whereas the second result considers that GCs are tidally stripped by their giant neighbors.

There are several processes that can produce tidal stripping of GCs. The main candidates are the pure gravitational forces due to the cluster potential well (see B2003), and the

galaxy-galaxy interaction (galaxy harassment). Using numerical simulations, Moore et al. (1996) demonstrated that in high mass galaxy cluster, this effect can indeed produce the stripping of an important part of the stellar component of galaxies. Based on the analysis of 228 elliptical galaxies in clusters, Cypriano et al. (2006) found that galaxies in the inner region of clusters are 5% smaller than those in the outer regions. This result is interpreted as evidence of the stripping of stars from elliptical galaxies in the central regions of clusters.

A precise knowledge of the number of GCs that galaxies could lose due to tidal stripping is particularly interesting for several reasons: i) If the models of GCs formation are going to be tested using observational data, GC population should be corrected by losses due to tidal stripping. ii) Some models for the formation and evolution of cD galaxies assume that a fraction of their GC population comes from tidal stripping of other cluster galaxy members (Forte et al. 1982, Hilker et al. 1999). The confirmation that tidal stripping is an efficient process will support this theory. iii) The GC population extends to large radii from the center of a galaxy. Therefore, GCs are ideal to study the outskirts of galaxies. If we can observe that GCs are being stripped by tidal interactions, this effect can be used to test a similar effect in other components of a galaxy, such as the dark matter halo.

In this work, we study the GC population of a sample of 13 member galaxies of the Virgo Cluster (VC). The ACS Virgo Cluster Survey (ACS VCS) is described in Côté et al. (2004) (hereafter C2004). There are many relevant papers produced by the ACS team: Color distributions of the GCs are presented in Peng et al. (2006); GC size distributions are analysed in Jordán et al. (2005); 3-dimensional distances for 84 galaxies in the VC are presented in Mei et al. (2007); surface brightness profiles, total magnitudes and colors of the sample galaxies are described in Ferrarese et al. (2006); specific frequency, GC number, T parameter, and other galaxy parameters are presented in P2008, while the GC catalogue used in the present work is described in Jordán et al. (2008). The aim of this paper is to detect whether there exist observational evidence of the tidal stripping effect on the GC population due to galaxy-galaxy interactions and/or by the cluster potential well. The paper is organized as follows: sample selection is described in Section 2, we discuss the GC selection in Section 2.2, while in Section 3, we derive and analyze our results; the final conclusions are summarized in Section 4.

2. The Sample

2.1. Galaxy Sample

The Virgo Cluster (VC) is a well studied cluster at a distance of 16.5Mpc (Tonry et al. 2001, Mei et al. 2007). It has a velocity dispersion of $776 \pm 21 \text{ km s}^{-1}$ (Girardi et al. 1993), and an intracluster gas temperature of 2.4 keV (David et al. 1993). Therefore, this cluster is an excellent candidate to study tidal stripping effects on the GC population. The ACS Virgo Cluster Survey is a dedicated optical and IR imaging survey of 100 Virgo’s early-type galaxies, which made use of the *Advanced Camera for Surveys* (ACS) on-board the *Hubble Space Telescope* (HST). These observations provide a unique opportunity to study GCs in cluster galaxies, as done by the ACS VCS team. They also provide an insight into the GC population in the intracluster medium (ICM). The complete survey is described in Côté et al. (2004) and data reduction techniques in Jordán et al. (2004). Briefly, the galaxies were observed through the F475W and F850LP filters that correspond to the Sloan g and z filters, respectively. The sample includes galaxies with $B_T < 16$ and they were required to have morphological types of E, S0, dE, dE,N, dS0 or dS0,N.

The number of GCs depends on the luminosity of the host galaxy. Moreover, the specific frequency S_N depends on the galaxy magnitude (Lotz et al. 2004, Miller & Lotz 2007, P2008). Since the ACS VCS sample spans over a wide luminosity range, and we want to avoid any luminosity bias in our analysis, we selected those galaxies with $-22.5 < M_z < -18.5$. Over this luminosity range, the specific frequency S_N and the T parameter (defined in Sect. 3) do not depend on the galaxy magnitude (P2008). On the other hand, since the GC population could depend on the host galaxy morphology, we have selected only elliptical galaxies. This type of galaxies shows (on average) the highest GC specific frequency for a given luminosity. In addition, we have only considered those elliptical galaxies that belong to the main cluster structure around M87 (Mei et al. 2007). The last criterion excludes VCC1178 and VCC1025 since they belong to the cluster sub-structure associated to M49. The sample comprises 13 elliptical galaxies located around M87. They span a range of galaxy projected distance to M87 between 0.04 and 1.65 Mpc, while their total absolute magnitudes satisfy that $-22.5 < M_z < -18.5$. Several galaxy properties, as the specific frequency S_N , T parameter and other properties, were taken from P2008. We have also used the 3-dimensional distances r_{3D} obtained by Mei et al. (2007). For our sample we obtain clustercentric distances $0.23 < r_{3D} < 2.0$. It should be taken into account that these distances have a line-of-sight uncertainties of ~ 0.6 Mpc. Mei et al. (2007) adopted the standard Λ CDM cosmology with $\Omega_m h^2 = 0.127^{+0.007}_{-0.013}$ and $h = 0.73 \pm 0.03$. Details of the 13 selected galaxies are quoted in Table 1.

2.2. Globular Cluster Selection

We specifically used the catalog of GC published by Jordán et al. (2008). This catalog contains 12763 bona-fide GC candidates which have the probability $p_{GC} > 0.5$ of being a GC according to their selection procedure. Basically, the selection procedure involves three main steps. The first one is described in Jordán et al. (2004) and contemplates the modeling and removal of the galaxy surface brightness distribution and subsequent object detection performed with SExtractor (Bertin & Arnouts 1996). In the second step all the GC candidates are run through the KINGPHOT code that fits PSF-convolved King models (King 1966) to their surface brightness profiles. Details about this code can be found in Jordán et al. (2005). Evaluated parameters for each GC candidate are: magnitude z (total and in a 0.2 arcsec diaphragm), celestial coordinates α and δ , half-light radius (r_h) and concentration defined as the logarithm of the core and tidal radii ratio. However, after the initial selection of GC candidates mentioned above there are still residual contaminants such as foreground stars and background galaxies. These residuals are removed in the third step. At this stage, they consider the data as a mixture of points drawn mainly from two populations, namely the GC and the contaminants. Thus, the data can be modeled using a mixture model with two component, in which the total observed distribution in the r_h - z plane is the result of summing these two components weighted by their respective sizes. The method follows the Fraley & Raftery (2002) procedure and it is also described in detail in Jordán et al. (2008).

3. Radial Dependencies

3.1. Density Profiles of Globular Clusters

The study of GCs around giant galaxies within clusters of galaxies has proved to be an useful tool for improving our knowledge about the formation and evolution of galaxies and their environments (Hanes et al. 2001; Côté et al. 2001, 2003).

The radial distributions of GCs are often fitted with a power law, which can be written as $\log(\rho) = \alpha \log(r) + \beta$ (Harris 1986, Ashman & Zepf 1998). Typically, power law indices range from ~ -2 to ~ -2.5 for low-luminosity Es (Harris & Harris 2001), and are ~ -1.5 for the most massive gEs. In general terms, blue metal-poor GCs present a shallower density profile than red GCs. Bassino et al. (2006) found that both density profiles, for blue and red GCs, can be well fitted using $\log(\rho) = ar^{1/4} + b$.

We have fitted a power law as well as $r^{1/4}$ law to our galaxy sample. GCs with $g - z >$

1.15 were considered metal rich (red GC), while GCs with $g - z < 1.15$ were considered metal poor (blue GC). The density profiles were computed using equal size bins (13.5 arcsec), therefore, the number of bins adopted in each galaxy depends on how far from the galaxy center we detected the GCs. In some cases only 3 bins were used, while in others up to 10 bins were considered. Error bars were estimated using the bootstrap resampling technique. In Table 2 the fitting parameters for all the galaxies are quoted. The mean value obtained to the slope α for all GCs is $\bar{\alpha} = -2.13 \pm 0.08$, while for red and blue GCs are $\bar{\alpha}_{red} = -2.4 \pm 0.2$ and $\bar{\alpha}_{blue} = -1.7 \pm 0.1$, respectively. Particularly, Fig. 1 shows the projected GC density profiles ($r^{1/4}$ law) for 4 galaxies of our sample. Left panels show the total GC density profiles, while right panels show the density profiles for the blue (squares) and red (triangles) GC populations separately. VCC1297 shows a flat density profile, therefore no profile was fitted, while VCC1422 does not present a red GC population. For the whole sample, we obtain a mean GC density profile with $\bar{a} = -1.59 \pm 0.06$, while for the red and blue GC populations the mean values are $\bar{a}_{red} = -1.8 \pm 0.1$, and $\bar{a}_{blue} = -1.22 \pm 0.07$, respectively. Several galaxies in our sample do not present bimodality in the color distribution of GCs (see Peng et al. 2006). Nevertheless, for most galaxies in our sample, red GC density profiles are steeper and more centrally concentrated than the corresponding blue GC density profiles. This could indicate that we indeed have two different GC populations.

Towards the inner region of the galaxy cluster, tidal effects are expected to become stronger due to a higher probability of encounters among galaxies, as well as the increase of the potential well. If we consider, in addition, that GCs located in the outskirts of galaxies are more prone to be stripped, then a correlation between the slope of the GC density profiles and the distance of hosts galaxies to M87 should be observed. This effect has already been reported by B2003 using numerical simulations. Nevertheless, for both, blue and red GCs, we do not find any correlation between these two parameters (see Fig. 2). A possible interpretation to this result is given in Sec. 4.

3.2. Specific Frequency S_N and T parameter

Harris & van den Bergh (1981) introduced the specific frequency S_N as a measure of GC richness normalized to the host galaxy luminosity:

$$S_N = N_{GC} 10^{0.4(M_V + 15)} \quad (1)$$

where N_{GC} is the total number of GCs and M_V is the V -band absolute magnitude. Typical values of S_N are ~ 1 for spirals and S0 galaxies (Barmby 2003), ~ 3 for ellipticals, and ~ 6 for cD galaxies (Ostrov et al. 1998). Nevertheless, the correlation between morphological types

and S_N contains some dispersion. On the other hand, several early studies suggest that S_N increases with galaxy luminosity (Miller et al. 1998, Lotz et al. 2001, Miller & Lotz 2007). However, P2008 found that the GC mass fraction is high in both giants and dwarfs galaxies, being universal in intermediate luminosity galaxies, while Strader et al. (2006) only found a weak signal in their $S_{N,B} - M_B$ data.

S_N can also depend on the environment, Ferguson & Sandage (1989) found that the number density of nucleated dwarf elliptical galaxies (dE) is more centrally concentrated than that of bright non-nucleated dE galaxies in the Virgo and Fornax Clusters. Miller & Lotz (2007) did not find a clear dependence of S_N on the environment for dEs. Using the VCS, P2008 found that galaxies within a projected radius of 1Mpc from M87 tend to have higher GC fractions, and this effect was interpreted in terms of the galaxy formation time. It should be noted that the described effect contradicts the tidal stripping scenario. Nevertheless, this result is observed when using the total sample of galaxies and does not discriminate by their luminosity, morphology or location Virgo’s sub-structures.

Panels (a) and (b) of Fig. 3 show S_N as a function of (r_p) and (r_{3D}) respectively for our sample of elliptical galaxies (see Table 1). We observe that larger S_N values are found at larger galaxy distances to M87 (\sim Virgo center). This result is indicating that the normalized number of GCs decreases as the host galaxy is closer to the Virgo center, where the tidal stripping is expected to be more efficient. A similar behavior is observed in panels (c) and (d), where we plot the specific frequency in the z bandpass $S_{N,z}$, as a function of the galaxy distances to M87. In the aforementioned Figure, panels (e),(f) and (g),(h) show the specific frequency $S_{N,z,blue}$ and $S_{N,z,red}$ versus galaxy distances to M87 for the blue and the red GC populations, respectively. It can be seen that both correlations, projected S_N vs. r_p and S_N vs. r_{3D} , are only present for the blue GC population. The lack of correlation for the red GCs could be explained by the fact that the distribution of red GC is more highly concentrated than the equivalent blue GC distribution, and therefore less affected by tidal effects. In order to quantify this effect, we split our sample into two: galaxies with $r_p < 0.8\text{Mpc}$ and $r_p > 0.8\text{Mpc}$. The adopted threshold for r_{3D} is 1.3Mpc (assuming that $r_{3D} = \sqrt{3}r_p$). For each sub-sample, the mean S_N are shown in Table 3. As it can be seen, galaxies in the outskirts of the Virgo cluster have mean S_N typically larger than those calculated for galaxies closer to M87. Particularly, we excluded VCC 1475 to compute the mean $S_{N,z,blue}$ and the mean T_{blue} due to its unexpected high values. Alternatively, for the blue GCs we fitted a linear regression between $S_{N,z,blue}$ and r_p and r_{3D} (see panels (e) and (f) in Fig. 3). Table 4 shows the fitting parameters, where it can be appreciated that fitted slopes differ from zero at six sigma levels. For the r_{3D} fits, we also excluded VCC 1475.

In addition, we show in Fig. 3, S_N vs. r_p (left panels) and S_N vs. r_{3D} (right panels),

discriminating the galaxy sample according to the absolute magnitude M_z of the galaxies. It can be appreciated that the correlation between S_N and r_p and r_{3D} is independent of the galaxy luminosity.

Using stellar masses of galaxies in the VCS, P2008 calculated the T parameter introduced by Zepf & Ashman (1993), defined as the number of GCs per $10^9 \mathcal{M}_\odot$,

$$T = \frac{N_{GC}}{\mathcal{M}_G/10^9 \mathcal{M}_\odot} \quad (2)$$

where \mathcal{M}_G is the stellar mass of the host galaxy. The use of T allows the comparison across galaxies with different mass-to-light-radius. Miller & Lotz (2007) and P2008 found that T correlates with galaxy luminosity, in the sense that higher T values correspond to brighter galaxies. Nevertheless, in the magnitude range of our sample, no correlation between T and the absolute magnitude is observed. Panels (a) and (b) of Fig. 4 show T vs. r_p and T vs. r_{3D} , respectively. Panels (c) and (d) correspond to the blue GC population for which we fitted a linear regression (again, the r_{3D} fit excludes VCC 1475), whereas panels (e) and (f) show the corresponding correlations for the red GCs. As it was observed for S_N , we only find correlations for the blue and the total GC populations. Higher values of T are found in the outskirts of the Virgo cluster (see also Tab. 3 and Tab. 4).

3.3. Local background of GCs

The observed population of GCs is superposed on a background contamination that exponentially grows with the apparent magnitude limit. This contamination is basically constituted by high redshift galaxies, foreground stars and a projected ICGC population. If tidal stripping of GCs is an efficient mechanism in clusters of galaxies, a fraction of the ICGC background would also be formed by stripped GCs. Moreover, this ICGC background would show a gradient, having higher values towards smaller projected clustocentric distances. There are several works that suggest the existence of the ICGC. West et al. (1995) suggested that the variation in the GC population in supergiant elliptical galaxies in clusters points towards the existence of a GC population that is not bound to any galaxy and moves throughout the core of the galaxy cluster. This was also suggested by Jordán et al. (2003) who used HST images of the rich cluster A1185. This galaxy cluster contains no bright galaxies, and shows an excess of point sources that is consistent with the existence of an ICGC population. The efficiency of GC tidal stripping due to the cluster potential well can be evaluated in terms of the tidal radii. Given a galaxy with mass \mathcal{M}_{gal} and at a given distance r_c from the cluster center, the tidal radius can be computed as

$$r_{tidal} = [G\mathcal{M}_{gal}/2v_{circ}^2]^{1/3} r_c^{2/3} \quad (3)$$

where v_{circ} is the circular velocity of the galaxy cluster potential. Therefore, for a typical elliptical galaxy with a total mass of $10^{12}M_{\odot}$ (Schindler et al. 1999), located in the VC potential, we obtain tidal radii of 11, 14 and 17 kpc for clustocentric distances of 0.2, 0.5 and 1.0 Mpc, respectively. These numbers indicate that if a galaxy passes close to the VC center it could lose part of its GC population due to tidal stripping.

Numerical simulations run by B2003 and BK2006 suggest that ICGCs are not necessarily uniformly distributed. GCs stripped from galaxies have not had enough time to be uniformly distributed in the IC medium. In fact, the simulation of B2003 shows that a fraction of the stripped GCs produces an enhancement in the local density around the parent galaxy. Moreover, BK2006 showed that, on average, ICGCs appear to have projected radial density profiles that grow towards the galaxy cluster centers. Based on these two results, we study the possible dependence of the ICGC population on the galaxy distance to M87. In our sample, we find that galaxies that are fainter than $M_z = -20.8$ (9 out of 13 galaxies) have a flat GC projected density profile for galactocentric distances greater than 1.3 arcmin (6.2 kpc). These galaxies are suitable to determine the local GC density around them since they have relatively small apparent diameters compared to the ACS field. We then calculated the local GC density beyond 6.2 kpc from the center of each of these galaxies. However, this density is still contaminated with high redshift galaxies and foreground stars. Hereafter we will refer to this local density as ρ_{out} .

P2008 determined fore- and background contamination using 10 blank fields images taken with the Wide Field Planetary Camera 2 (WFPC2). They found that there are on average 5.8 ± 2.5 contaminants sources per WFPC2 field. We use this number to estimate the contribution of the mean fore- and background contamination to ρ_{out} . Figure 5 shows the total, blue and red (from top to bottom) local density ρ_{out} around the selected nine galaxies as function of r_p (left panels) and r_{3D} (right panels). Error bars were estimated using the bootstrap resampling technique. Horizontal dashed lines correspond to the mean value of ρ_{out} computed for those galaxies with clustocentric distances $r_p > 100$ kpc. These values are 2.4 ± 0.3 (arcmin⁻²) for all GCs, 1.7 ± 0.3 for blue GCs, and 0.6 ± 0.2 for red GCs. Horizontal dotted lines show the mean density (blue and red) of the fore- and background contaminants derived by P2008 from 10 blank fields (1.1 ± 0.5). It can be seen that nine (eight) galaxies have values of ρ_{out} for the total (blue) GC population consistent or higher than expected mean values of the fore- and background contaminants. Except for two galaxies, the values of ρ_{out} for the red GC population, are lower than the expected for the total mean fore- and background contamination. On the other hand, we found for the total and blue GC populations, that three galaxies (VCC1297, VCC1279 and VCC0828) have ρ_{out} values three times larger than the contaminants mean density. The same figure also shows that the two highest values of ρ_{out} correspond to the galaxies with the lowest values of S_N (VCC1297 and

VCC1279) that are also the galaxies closest to M87 (see Table 1), which has an extended halo of GCs. The extended GC halo of M87 could be partially contributing to the high density levels observed around these two galaxies. However, since M87 is located near the center of the cluster potential well we are unable to determine if this additional contribution is derived from GCs bound to M87 itself, or if they are truly ICGCs. In any case, the procedure we use to compute the background is independent of the origin of GCs and therefore, our method does accurately represent the GC background around these galaxies.

4. Conclusions and Discussion

We analysed a sample of 13 elliptical galaxies taken from the ACS VCS with the aim of finding evidence of the tidal stripping of GCs. Particularly, we focused our attention on the dependence of several galaxy properties with the radial clustocentric distance. The selected sample comprises host galaxies in the magnitude range $-22.5 < M_z < -18.5$ that belong to the main concentration of the VC. The GCs around these galaxies were taken from Jordán et al. (2008), while several galaxy properties were taken from P2008. The color index $g - z$ was used to discriminate metal poor (blue) from metal rich (red) GCs.

There is a correlation between the specific frequency, in the V and z -bands, and the galaxy distances to M87. Larger values of S_N are found at larger clustocentric distances. The effect is observed using both projected or 3-dimensional distances. If GCs are selected according to their color, the correlation is only observed in the blue (metal poor) population. These results are in agreement with the idea that those galaxies closer to the Virgo center are losing a fraction of their GCs due to tidal stripping. The lack of correlation for the red GC (metal rich) population could be explained if we consider that these objects have a more concentrated distribution around the host galaxy, and therefore they are less affected by tidal effects than the blue GCs. Similarly, we found a correlation between the T parameter (the number of GCs normalized to galaxy stellar mass) and r_p and T and r_{3D} , for the total and blue GC populations only. T increases as the galaxy distance to M87 increases. The lowest values of S_N and T are found within 100kpc to the cluster center, where P2008 have also reported evidences of tidal stripping.

As it was explained before, P2008 found that: a) S_N and T depend on the environment, i.e. galaxies within a projected radius of 1 Mpc from the cluster center tend to have higher GC fractions than galaxies at larger clustocentric distances. b) Galaxies within $r_p \simeq 40$ kpc from M87 (and M49) have a few or no GCs. The first result is interpreted in terms of formation time. GC formation in centrally located low-mass galaxies is biased because their stars form earlier. The second result considers that GCs are tidally stripped from the parent

galaxies by their giant neighbors. At first glance, our findings appear to differ from the aforementioned P2008 result (a), since we find that the mean S_N value is indeed higher at larger r_p . Nevertheless, before we can compare our results to those of P2008 we have to consider the following: i) although all VCC galaxies are early-types, P2008 analysed the radial dependence for a great variety of galaxy morphologies, while our analyses only consider pure elliptical galaxies; ii) our sample excludes bright and faint VCC galaxies and comprises only those objects in the magnitude range $-22.5 < M_z < -18.5$, for which P2008 data show no correlation between the galaxy magnitude and S_N . This is the most important difference between our analysis and that performed by P2008, since the dependences of S_N and T on the galaxy magnitude tend to erase any other correlation; iii) our study only considers galaxies that belong to the main concentration around M87 and excludes galaxies close to M49. It is more likely that the dynamic history of these galaxies is more related to the group of M49 than to the Virgo cluster.

We tested a possible correlation between the slopes of the GC density profiles and the clustocentric distances as predicted by B2003 numerical simulations. Computed slopes for our galaxy sample do not show correlation with r_p nor with r_{3D} . Cypriano et al. (2006) found that galaxies in the inner regions of clusters are 5% smaller than those in the outer regions. These authors interpret this result in terms of star stripping. Aguilar & White (1986, 1987) studied this effect using numerical simulations and they found that the $r^{1/4}$ luminosity profile is robust, since it is recovered after the galaxy interaction or merger. However, $r^{1/4}$ parameters, the effective radius r_e and the surface brightness μ_e inside r_e , change depending on the collision type. Strong collisions result in a reduced r_e and a higher μ_e , while weak collisions produce the opposite effect. If GCs are affected by the same process that affect the stars, the GC distribution could also be modified, but the final density profile will also depend on the interaction class. If this model is correct, no correlation between the slopes of the GC distribution and the clustocentric distances should be expected.

We also computed the GC density ρ_{out} , outside 6.2 kpc from the galaxy center for nine galaxies of our sample. Our results show that values of ρ_{out} for the total (blue) GC population around nine (eight) of the selected fields are consistent, or larger, than those expected from the fore and background contaminants. Except for two of the nine selected fields, the values of ρ_{out} for the red GC population are lower than expected for the mean fore- and background contamination. These results indicate that the ICGC population around most of the galaxies of our sample is mainly composed of blue GC. The two highest values of ρ_{out} (that correspond to the two lowest values of S_N) are found in the core of the VC (within 100kpc), confirming P2008 results. They could be stripped GCs from neighbor galaxies, some fraction of the very extended GC distribution of M87, and/or a genuine ICGC population. The two fields at larger clustocentric distances with total and blue values of ρ_{out} larger than expected for

the fore- and background contamination could be either a cosmic variance or the result of GCs stripped from the parent galaxy that have not had enough time to uniformly distribute into the intracluster medium.

The evidence for tidal stripping found in this work suggests that special care should be taken in studies that attempt to model the formation and evolution of the GC population. The number, proportion and distribution of GCs observed in those elliptical galaxies close to the center in a massive cluster, appear to significantly differ from the GC population in galaxies before they approached the center of the cluster. Moreover, a good estimate of the background contamination in GC counts is critical, since we have shown the possible existence of both, a mean gradient as a function of r_p , and a possible cosmic scatter of the mean local background around some galaxies. Finally, more realistic simulations are needed in order to confront observational results with model predictions. A complete set of cluster galaxies selected from a cosmological simulation should be analyzed. Besides, metal poor and metal rich GCs with their corresponding radial distributions should be considered. Simulations constrained in this way, have the potential to predict the initial undisturbed radial distribution of GCs around galaxies in rich clusters.

5. Acknowledgments

We kindly thank Sebastian Gurovich and Eugenia Díaz for their helpful comments on the manuscript. We are grateful to the referee for his valuable comments, which contribute to improve the present paper. HM thanks Juan Carlos Forte and Favio Faifer for the useful discussions. This work was partially supported by the Consejo de Investigaciones Científicas y Técnicas de la República Argentina, CONICET; SeCyT, UNC, Agencia Nacional de Promoción Científica, Argentina. Support for this work was provided by the National Science Foundation through grant N1183 from the Association of Universities for Research in Astronomy, Inc., under NSF cooperative agreement AST-0132798.

REFERENCES

- Aguilar, L. A., & White, S. D. M. 1986, *ApJ*, 307, 97
- Aguilar, L. A., & White, S. D. M. 1987, in *IAU Symposium*, Vol. 127, *Structure and Dynamics of Elliptical Galaxies*, ed. P. T. de Zeeuw, 517–+

- Ashman, K. M., & Zepf, S. E. 1998, *Globular Cluster Systems* (Globular cluster systems / Keith M. Ashman, Stephen E. Zepf. Cambridge, U. K. ; New York : Cambridge University Press, 1998. (Cambridge astrophysics series ; 30) QB853.5 .A84 1998 (\$69.95))
- Barmby, P. 2003, in *Extragalactic Globular Cluster Systems*, ed. M. Kissler-Patig, 143–+
- Bassino, L. P., Faifer, F. R., Forte, J. C., Dirsch, B., Richtler, T., Geisler, D., & Schuberth, Y. 2006, *A&A*, 451, 789
- Bekki, K., Forbes, D. A., Beasley, M. A., & Couch, W. J. 2003, *MNRAS*, 344, 1334
- Bekki, K., & Yahagi, H. 2006, *MNRAS*, 372, 1019
- Bertin, E., & Arnouts, S. 1996, *A&AS*, 117, 393
- Côté, P., et al. 2004, *ApJS*, 153, 223
- Côté, P., Marzke, R. O., & West, M. J. 1998, *ApJ*, 501, 554
- Côté, P., McLaughlin, D. E., Cohen, J. G., & Blakeslee, J. P. 2003, *ApJ*, 591, 850
- Côté, P., et al. 2001, *ApJ*, 559, 828
- Cypriano, E. S., Sodr e, L. J., Campusano, L. E., Dale, D. A., & Hardy, E. 2006, *AJ*, 131, 2417
- David, L. P., Slyz, A., Jones, C., Forman, W., Vrtilik, S. D., & Arnaud, K. A. 1993, *ApJ*, 412, 479
- Ferguson, H. C., & Sandage, A. 1989, *ApJL*, 346, L53
- Ferrarese, L., et al. 2006, *ApJS*, 164, 334
- Forbes, D. A., Brodie, J. P., & Grillmair, C. J. 1997, *AJ*, 113, 1652
- Forte, J. C., Martinez, R. E., & Muzzio, J. C. 1982, *AJ*, 87, 1465
- Fraley, C., & Ratftery, A. 2002, *Jour. Am. Stat. Assoc.*, 97, 611
- Girardi, M., Biviano, A., Giuricin, G., Mardirossian, F., & Mezzetti, M. 1993, *ApJ*, 404, 38
- Hanes, D. A., C t e, P., Bridges, T. J., McLaughlin, D. E., Geisler, D., Harris, G. L. H., Hesser, J. E., & Lee, M. G. 2001, *ApJ*, 559, 812
- Harris, W. E. 1986, *AJ*, 91, 822

- Harris, W. E., & Harris, G. L. H. 2001, *AJ*, 122, 3065
- Harris, W. E., & van den Bergh, S. 1981, *AJ*, 86, 1627
- Hilker, M., Infante, L., & Richtler, T. 1999, *A&AS*, 138, 55
- Jordán, A., et al. 2004, *ApJS*, 154, 509
- Jordán, A., Côté, P., Blakeslee, J. P., Ferrarese, L., McLaughlin, D. E., Mei, S., Peng, E. W., & et al. 2005, *ApJ*, 634, 1002
- Jordán, A., Peng, E.W., B. J. P., & et al. 2008, *ApJS* accepted, in press
- Jordán, A., West, M. J., Côté, P., & Marzke, R. O. 2003, *AJ*, 125, 1642
- King, I. R. 1966, *AJ*, 71, 64
- Lotz, J. M., Miller, B. W., & Ferguson, H. C. 2004, *ApJ*, 613, 262
- Lotz, J. M., Telford, R., Ferguson, H. C., Miller, B. W., Stiavelli, M., & Mack, J. 2001, *ApJ*, 552, 572
- Mei, S., et al. 2007, *ApJ*, 655, 144
- Miller, B. W., & Lotz, J. M. 2007, *ApJ*, 670, 1074
- Miller, B. W., Lotz, J. M., Ferguson, H. C., Stiavelli, M., & Whitmore, B. C. 1998, *ApJL*, 508, L133
- Moore, B., Katz, N., Lake, G., Dressler, A., & Oemler, A. 1996, *Nature*, 379, 613
- Muzzio, J. C. 1986, *ApJ*, 301, 23
- Muzzio, J. C., Dessaunet, V. H., & Vergne, M. M. 1987, *ApJ*, 313, 112
- Ostrov, P. G., Forte, J. C., & Geisler, D. 1998, *AJ*, 116, 2854
- Peng, E. W., et al. 2006, *ApJ*, 639, 95
- Peng, E. W., Jordán, A., Côté, P., & et al. 2008, *ApJ*, 681, 197
- Schindler, S., Binggeli, B., & Böhringer, H. 1999, *A&A*, 343, 420
- Strader, J., Brodie, J. P., Spitler, L., & Beasley, M. A. 2006, *AJ*, 132, 2333

Tonry, J. L., Dressler, A., Blakeslee, J. P., Ajhar, E. A., Fletcher, A. B., Luppino, G. A., Metzger, M. R., & Moore, C. B. 2001, *ApJ*, 546, 681

West, M. J., Cote, P., Jones, C., Forman, W., & Marzke, R. O. 1995, *ApJL*, 453, L77+

Zepf, S. E., & Ashman, K. M. 1993, *MNRAS*, 264, 611

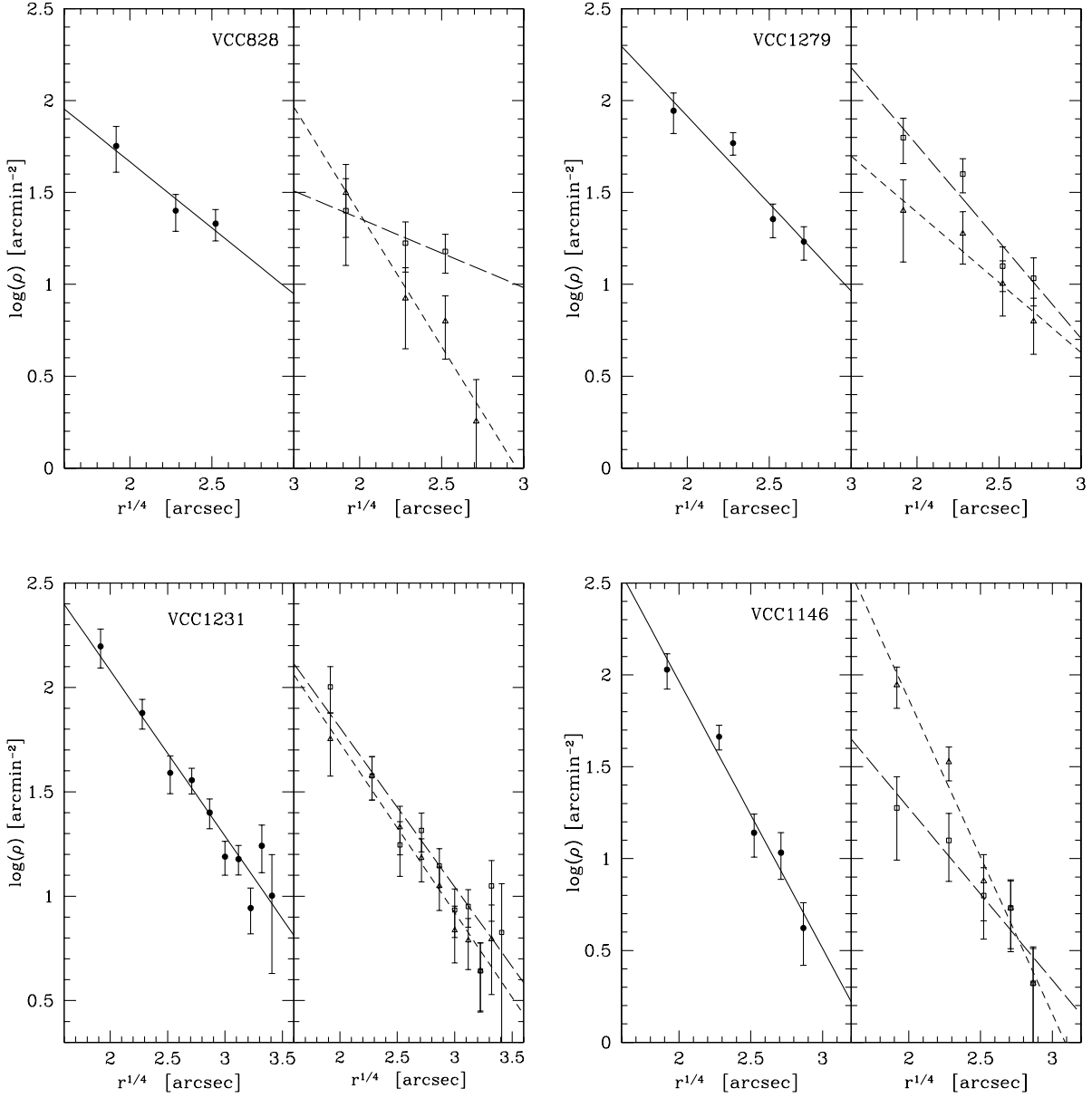


Fig. 1.— GC projected density profiles for four galaxies in our sample. Filled squares, open triangles and open squares correspond to the total, red and blue GC, respectively. *Long dashed lines* and *short dashed lines* correspond to $r^{1/4}$ fit for the blue and the red GC population, respectively. Errors bars were estimated using the bootstrap resampling technique.

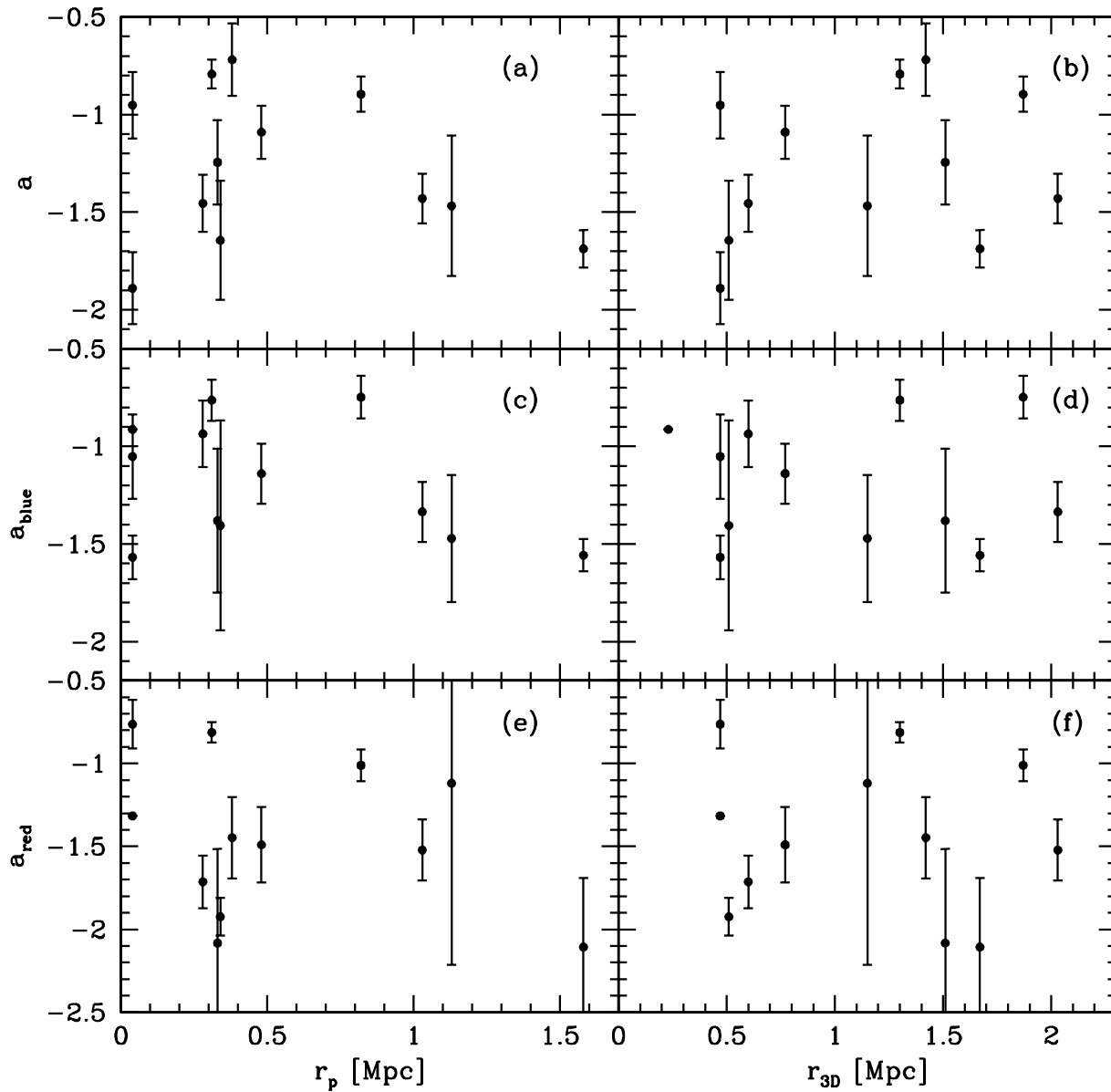


Fig. 2.— Slopes of the GC projected density profiles as a function of the galaxy projected distance r_p (*left panels*) and as a function of the galaxy 3-dimensional distance r_{3D} to M87 (*right panels*). *From top to bottom*: correlations for the total GC population, blue and red GC populations.

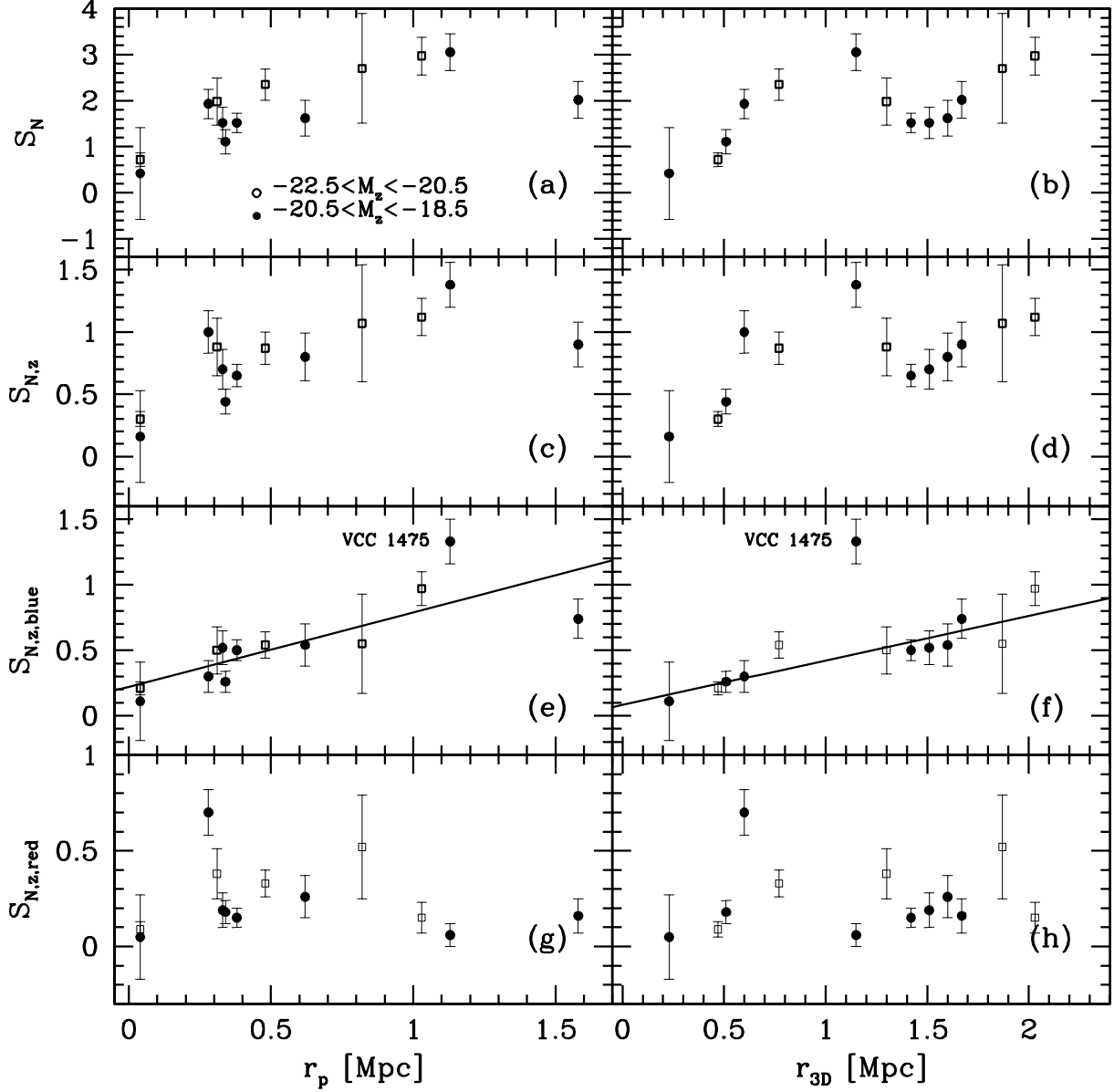


Fig. 3.— S_N of each galaxy as a function of the clustocentric projected distance r_p of the host galaxy (*left panels*) and as a function of the galaxy 3-dimensional distance r_{3D} (*right panels*). *From top to bottom*: correlations for the total GC population in V-band, total GC population in the z -band, blue GC population in the z -band and red GC population in the z -band. *Black solid lines* in panels e) and f) correspond to linear regressions. *Open and solid symbols* consider two different ranges in the absolute magnitude M_z of the host galaxy.

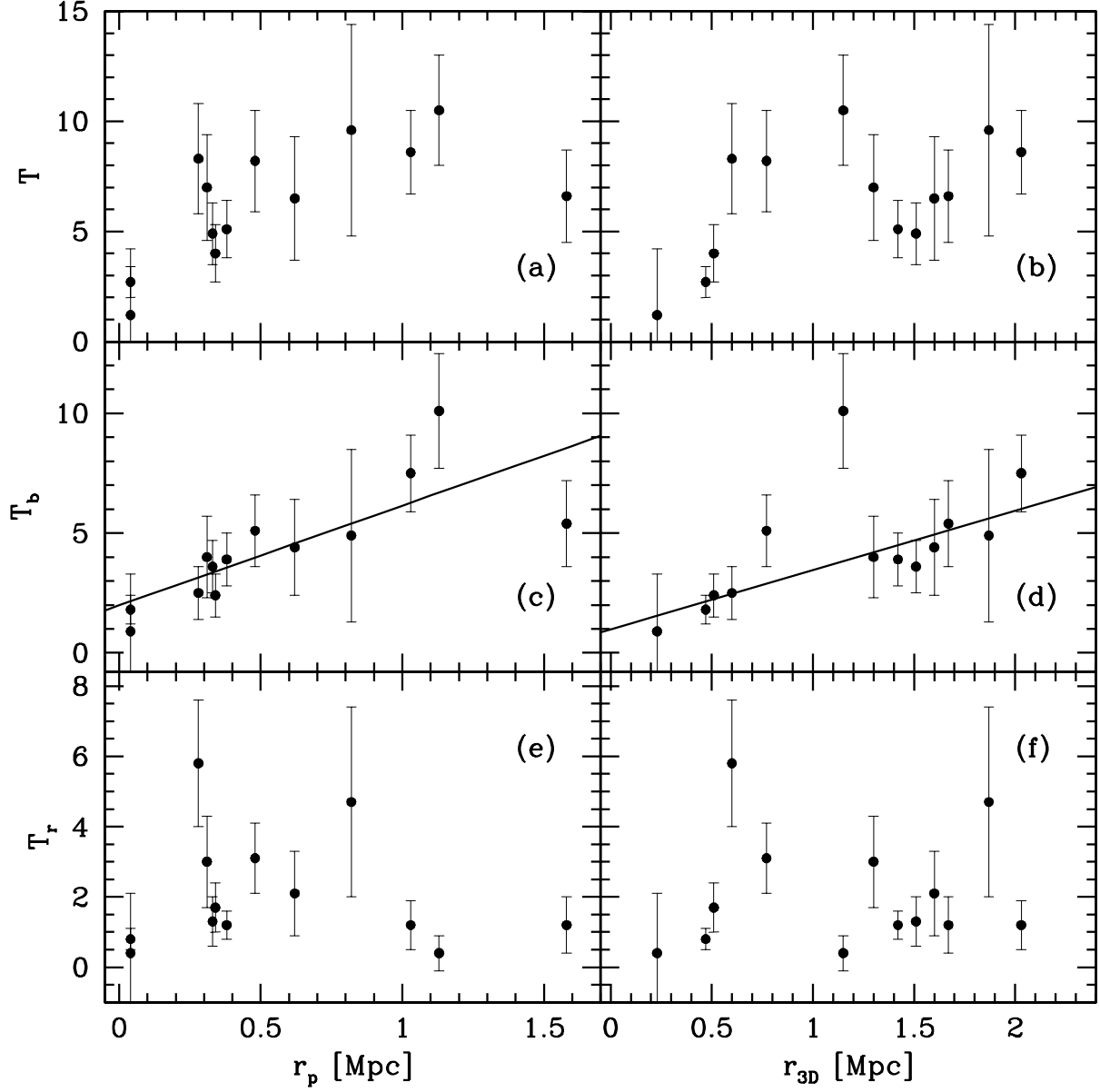


Fig. 4.— Some as Fig. 2 but now for the T parameter.

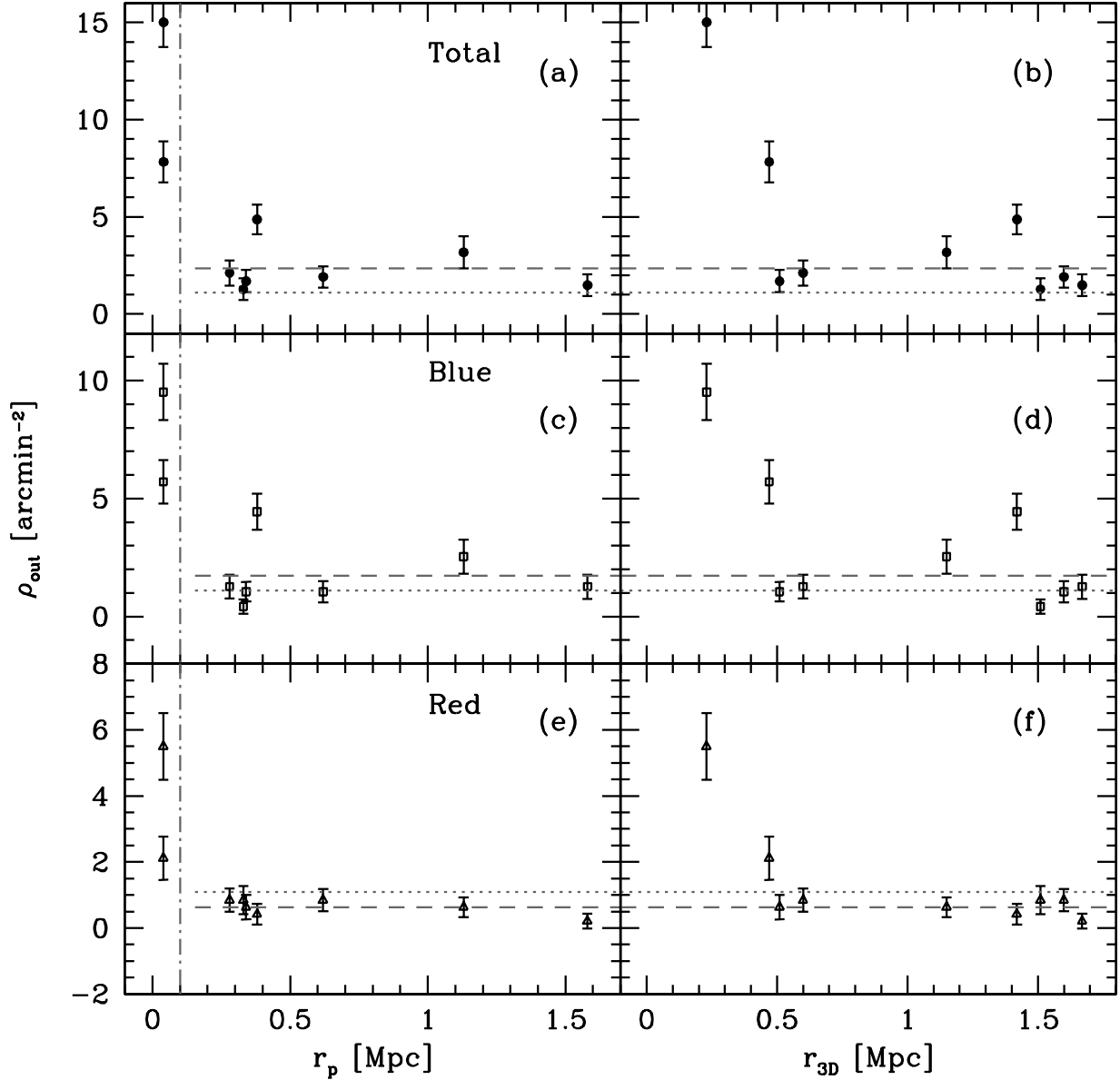


Fig. 5.— Total local density ρ_{out} as a function of the distance to M87, from top to bottom: for the total GC population, blue GC population and red GC population. *Black solid lines* in panels e) and f) correspond to linear regressions. The horizontal dashed lines correspond to the mean total density computed around galaxies at $r_p > 100$ kpc (*vertical lines*). Dotted lines show the expected mean density of the fore- and background contaminants. Errors bars were estimated using the bootstrap resampling technique.

Table 1. Galaxy properties in ACS Virgo Cluster Survey taken from Peng et al. (2008) and Mei et al. (2007).

VCC (1)	M_z (2)	r_p (3)	r_{3D} (4)	N_{GC} (5)	S_N (6)	$S_{N,z}$ (7)	$S_{N,z,blue}$ (8)	$S_{N,z,red}$ (9)	T (10)	T_{blue} (11)	T_{red} (12)	Type (13)
1903	-22.19	0.82	1.87 ± 0.35	803 ± 355	2.71 ± 1.19	1.07 ± 0.47	0.55 ± 0.38	0.52 ± 0.27	9.6 ± 4.8	6.2 ± 2.0	4.1 ± 1.4	E5
1231	-21.58	0.31	1.30 ± 0.36	376 ± 97	1.98 ± 0.51	0.88 ± 0.23	0.50 ± 0.18	0.38 ± 0.13	7.0 ± 2.4	4.0 ± 1.7	3.0 ± 1.3	E5
2000	-20.66	1.03	2.03 ± 0.35	205 ± 28	2.97 ± 0.41	1.12 ± 0.15	0.97 ± 0.13	0.15 ± 0.08	8.6 ± 1.9	7.5 ± 1.6	1.2 ± 0.7	E5
1664	-20.97	0.48	0.77 ± 0.38	213 ± 31	2.35 ± 0.34	0.87 ± 0.13	0.54 ± 0.10	0.33 ± 0.07	8.2 ± 2.3	5.1 ± 1.5	3.1 ± 1.0	E6
1279	-20.72	0.04	0.47 ± 0.40	58 ± 11	0.72 ± 0.15	0.30 ± 0.06	0.21 ± 0.15	0.09 ± 0.04	2.7 ± 0.7	1.8 ± 0.6	0.8 ± 0.3	E2
1619	-20.19	0.33	1.51 ± 0.36	84 ± 19	1.52 ± 0.34	0.70 ± 0.16	0.52 ± 0.13	0.19 ± 0.09	4.9 ± 1.4	3.6 ± 1.1	1.3 ± 0.7	E/S0
0828	-20.07	0.38	1.42 ± 0.42	69.5 ± 9.8	1.52 ± 0.21	0.65 ± 0.09	0.50 ± 0.08	0.50 ± 0.08	5.1 ± 1.3	3.9 ± 1.1	1.2 ± 0.4	E5
1630	-22.19	0.82	1.87 ± 0.35	47 ± 11	1.11 ± 0.26	0.44 ± 0.10	0.26 ± 0.08	0.18 ± 0.06	4.0 ± 1.3	2.4 ± 0.9	1.7 ± 0.7	E
1146	-20.06	0.34	0.51 ± 0.38	72 ± 12	1.93 ± 0.32	1.00 ± 0.17	0.30 ± 0.12	0.70 ± 0.12	8.3 ± 2.5	2.5 ± 1.1	5.8 ± 1.8	E
1913	-19.74	1.58	1.67 ± 0.40	71 ± 14	2.02 ± 0.40	0.90 ± 0.18	0.74 ± 0.15	0.16 ± 0.09	6.6 ± 2.1	5.4 ± 1.8	1.2 ± 0.8	E
1475	-19.42	1.13	1.15 ± 0.38	81 ± 10	3.05 ± 0.40	1.38 ± 0.18	1.33 ± 0.17	0.06 ± 0.06	10.5 ± 2.5	10.1 ± 2.4	0.4 ± 0.5	E
1422	-18.73	0.62	1.60 ± 0.43	24.9 ± 6.0	1.62 ± 0.39	0.80 ± 0.19	0.54 ± 0.16	0.26 ± 0.11	6.5 ± 2.8	4.4 ± 2.0	2.1 ± 1.2	E
1297	-18.75	0.04	0.23 ± 0.46	4 ± 11	0.42 ± 1.00	0.16 ± 0.37	0.11 ± 0.30	0.05 ± 0.22	1.2 ± 3.0	0.9 ± 2.4	0.4 ± 1.7	E

Note. — (1) Number in Virgo Cluster Catalog. (2) Absolute z magnitude. (3) Projected distance from M87, in Mpc. (4) 3-dimensional distance from M87, in Mpc. (5) Total number of GCs. (6) Specific frequency in V -band. (7) Specific frequency in z bandpass. (8) Specific frequency in z for blue GCs. (9) Specific frequency in z for red GCs. (10) T parameter: N_{GC} normalized to stellar mass of $10^9 M_{\odot}$. (11) T parameter to blue GCs. (12) T parameter to red GCs. (13) Morphological type.

Table 2. Fit parameters of density profiles.

VCC	a	a_{blue}	a_{red}	α	α_{blue}	α_{red}
1903	-0.90 ± 0.09	-0.7 ± 0.1	-1.0 ± 0.1	-1.3 ± 0.2	-1.1 ± 0.2	-1.4 ± 0.2
1231	-0.79 ± 0.07	-0.8 ± 0.1	-0.81 ± 0.06	-1.2 ± 0.1	-1.2 ± 0.1	-1.2 ± 0.1
2000	-1.4 ± 0.1	-1.3 ± 0.2	-1.5 ± 0.2	-2.1 ± 0.3	-2.0 ± 0.3	-2.1 ± 0.3
1664	-1.1 ± 0.1	-1.1 ± 0.2	-1.5 ± 0.2	-1.7 ± 0.2	-1.7 ± 0.2	-2.1 ± 0.4
1279	-1.0 ± 0.2	-1.1 ± 0.2	-0.8 ± 0.1	-1.2 ± 0.3	-1.4 ± 0.3	-1.0 ± 0.2
1619	-1.02 ± 0.2	-1.4 ± 0.4	-2.1 ± 0.7	-1.7 ± 0.3	-1.9 ± 0.5	-2.6 ± 0.8
0828	-0.7 ± 0.2	-0.38 ± 0.08	-1.4 ± 0.2	-0.9 ± 0.2	-0.48 ± 0.09	-1.9 ± 0.4
1630	-1.6 ± 0.3	-1.4 ± 0.5	-1.9 ± 0.1	-2.1 ± 0.4	-1.8 ± 0.7	-2.5 ± 0.2
1146	-1.5 ± 0.1	-0.9 ± 0.1	-1.7 ± 0.2	-1.9 ± 0.2	-1.2 ± 0.3	-2.3 ± 0.3
1913	-1.7 ± 0.1	-1.56 ± 0.08	-2.1 ± 0.4	-2.4 ± 0.1	-2.1 ± 0.1	-2.8 ± 0.5
1475	-1.5 ± 0.4	-1.5 ± 0.3	-1 ± 1	-1.9 ± 0.5	-1.9 ± 0.5	-1.4 ± 1.5
1422	-1.9 ± 0.2	-1.6 ± 0.1	...	-2.5 ± 0.3	-1.99 ± 0.07	...
1297
<i>mean values</i>	-1.59 ± 0.06	-1.22 ± 0.07	-1.8 ± 0.1	-1.13 ± 0.08	-1.7 ± 0.1	-2.4 ± 0.2

Table 3. Mean values of S_N and T as a function of r_p and r_{3D} .

	$r_p < 0.8 \text{ Mpc}$	$r_p > 0.8 \text{ Mpc}$	$r_{3D} < 1.3 \text{ Mpc}^a$	$r_{3D} > 1.3 \text{ Mpc}$
S_N	1.5 ± 0.2	2.4 ± 0.3	1.8 ± 0.2	2.0 ± 0.4
$S_{N,z}$	0.67 ± 0.07	1.0 ± 0.1	0.78 ± 0.06	0.9 ± 0.2
$S_{N,z,blue}^b$	0.40 ± 0.06	0.77 ± 0.09	0.45 ± 0.06	0.7 ± 0.2
$S_{N,z,red}$	0.3 ± 0.04	0.2 ± 0.06	0.28 ± 0.04	0.2 ± 0.09
T	5.5 ± 0.3	8 ± 1	6.4 ± 0.7	7 ± 2
T_{blue}^b	3.3 ± 0.5	6.3 ± 0.8	3.8 ± 0.5	5 ± 2
T_{red}	2.2 ± 0.3	1.7 ± 0.4	2.1 ± 0.3	1.2 ± 0.8

^a1.3Mpc correspond to $r_{3D} \sim 0.8\sqrt{3}\text{Mpc}$.

^bIn the r_{3D} analysis, we excluded VCC1475 (see the text).

Table 4. Parameters of the linear fit of $S_{N,z,blue}$ and T_{blue} as function of r_p and r_{3D} . a is the slope and b the zeropoint.

		r_p	r_{3D}
$S_{N,z,blue}$	a	0.6 ± 0.1	0.34 ± 0.06
	b	0.2 ± 0.1	0.08 ± 0.07
T_{blue}	a	4 ± 1	2.5 ± 0.5
	b	2.0 ± 0.7	1.0 ± 0.6